Article

Hydrodynamic Effects on Spectroscopic Water Detection in Gasoline Pipe Flow

Jeong Heon Kim [1] and Chang Sik Lee [2],*

[1] R&D Division, IGT Corporation, 403 Industry Academy Collaboration Center, Kongju National University, 1223-24 Cheonandaero, Seobukgu, Cheonansi, Chungnam 331-717, Korea; E-Mail: jnvr@naver.com

[2] School of Mechanical Engineering, Hanyang University, 222 Wangsimni-ro, Seongdong-gu, Seoul 133-791, Korea

* Author to whom correspondence should be addressed; E-Mail: cslee@hanyang.ac.kr; Tel.: +82-2-2220-0427; Fax: +82-2-2281-5286.

Abstract: The hydrodynamic effects on spectroscopic water detection were microscopically investigated in a gasoline pipe flow. The effects of the gasoline flow rate and the water content on the water droplet characteristics were investigated experimentally using a phase Doppler particle measurement system. The characteristics of spectral absorbance of water and gasoline were measured using a spectrophotometer to determine the optimal wavelength of the incident light for spectroscopic water detection. The effects of the droplet size on the light transmittance characteristics were calculated using the light extinction theory of Mie scattering on polydisperse particles and experimental results on the water droplet size in the gasoline flow. The measurement results of spectral absorbance showed that gasoline was almost transparent at 980 nm wavelength of light while water showed peak absorption at this wavelength, therefore, it was appropriate incident light for spectroscopic water detection. It was found that the flow conditions of the gasoline flow rate and the water content influenced the Sauter mean diameter and the volume concentration of water droplets, which influenced the light transmittance.

Keywords: spectroscopic water detection; light transmittance and absorbance; hydrodynamic break-up; phase Doppler measurement

1. Introduction

The water content in a liquid petroleum fuel is an influential factor in determining the fuel quality because the fuel composition is contaminated by water. The permissible water content in gasoline is generally limited to a very small amount of about 100 ppm. The instantaneous water detection in a gasoline pipelines is very useful to control the quality and purity of the fuel. Many studies on the water content in liquid fuel have been reported over the years and most of these researches have investigated the performance and emissions of combustion engine systems [1–5]. However, few studies on the microscopic characteristics of water droplets in a liquid fuel have been reported [6–8]. Chantrapornchai *et al*. [6] studied the influences of droplet characteristics on the optical properties of oil-in-water emulsions containing different colored dyes. Bampi *et al*. [8] used near-infrared spectroscopy to predict the droplet size and water content in a soybean and animal fat biodiesel emulsion. In their work, NIR spectroscopy was confirmed to be a good option to estimate the average droplet size and water content in water-biodiesel emulsions.

The water component can be measured using spectroscopy technology which is the most accurate technique in the microanalysis of material components. Applying spectroscopy techniques to an optical monitoring system can be considered for quality management. However, practical applications of the spectroscopy technique to a gasoline pipe flow are very difficult because the optical characteristics can be affected by water droplet characteristics in the flow field [9,10].

The purpose of this paper is to investigate the hydrodynamic effects on spectroscopic water detection in a gasoline pipe flow. The effects of the gasoline flow rate and the water content on the water droplet characteristics were experimentally investigated by using the phase Doppler particle measurement system. The spectral absorbance characteristics of water and gasoline were measured by a spectrophotometer to determine the optimal wavelength of the incident light for spectroscopic water detection. The effects of the water droplet characteristics on the light transmittance in the gasoline pipe flow were calculated using the approximate light extinction theory of Mie scattering on polydisperse particles and the experimental results of the water droplet size.

2. Experimental Setup and Procedures

2.1. Experimental Apparatus

The experimental system for measurement of water droplet characteristics in the gasoline pipe flow was set up as shown in Figure 1. It was composed of a stainless steel pipeline with transparent test windows, gasoline and water supply systems, and a mixing device. The flow rates of gasoline and water were controlled with a control valve and the nitrogen gas pressure of the water supply tank, respectively. Water was supplied through a supply nozzle with a diameter of 0.2 mm and was mixed with gasoline through a mixing device, which was composed of two meshes with a cell size of 74 µm and installed downstream of the water nozzle. A rectangular pipe of 28 mm × 28 mm was used as a gasoline pipeline and was designed to allow detection of the optical measurements through the transparent windows as shown in Figure 1. The behavior of water droplets injected from the nozzle was observed at test window 1 and the water droplet characteristics were measured at test window 2. The distance between the mixing device and test Section 2 was 2 m, which was about 70 times of the

hydraulic diameter of the gasoline pipe. The water injected from the nozzle disintegrated into small droplets by a hydrodynamic atomization through the mixing device and small droplets dispersed spatially in the gasoline pipeline as shown in Figure 1. The gasoline flow rate varied with the range of $Q_g = 1.8–3.6$ m^3/h, which is corresponded to a turbulent flow in the range of Reynolds numbers $Re_g = 40{,}000–80{,}000$. The water content was varied in the range of $C_w = 50–250$ ppm under consideration of the gasoline quality regulation.

Figure 1. Schematic diagram of experimental setup.
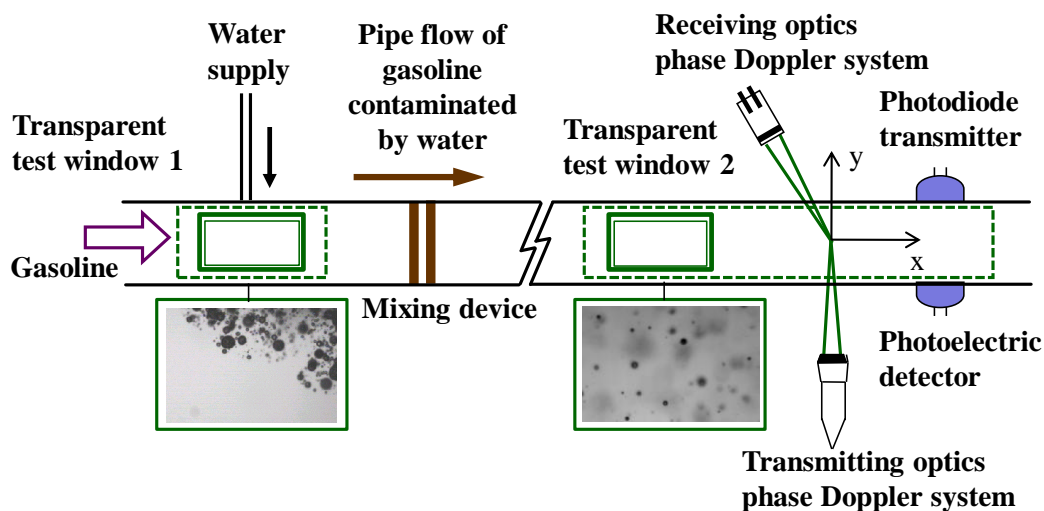
2.2. Phase Doppler Particle Measurement System

The size and velocity of water droplets were simultaneously measured using a phase Doppler particle measurement system. The phase Doppler measurement technique is one of the most versatile and accurate techniques currently available for simultaneous measurements of the size and velocity of droplets. The coherent light from a laser is separated into two beams and focused by a converging lens. Interference fringes appear in the intersection volume of the two beams. The light scattered by a particle crossing the measurement volume features a periodic signal, which is the Doppler signal with a frequency proportional to the velocity of particles and to the inverse of the fringe interval. This interval is constant and depends on the geometry of the optical set-up and the wavelength of the laser. If the scattered light is observed from two different angles of two photo-multipliers, two Doppler signals with different phases can be detected. The difference is proportional to a droplet diameter. Thus, the diameter and velocity of droplets can be measured simultaneously [11–13].

A one-dimensional phase Doppler anemometer system was used for simultaneous measurement of the velocity and diameter of water droplets. The optical configurations of phase Doppler measurements were optimized for this experiment. The light source was an argon-ion laser and a wavelength of 514.5 nm (green) was used for velocity and diameter. The light power of the two laser beams was 70 mW, and the frequency shift was 40 MHz. The scattering angle was 30 degrees, which was determined by considering the polarizing angle and the refractive index. The focal lengths of the transmitting and receiving lenses were 250 mm and 310 mm, respectively, in order to optimize the measurement volume and the measurement range. The resolution of the droplet diameter was

0.955 µm/degree. The measured droplet was regarded as a valid sample when the droplet sphericity was over 90%. The sphericity was determined from two diameters, d_1 and d_2 measured by three photomultipliers with each different angle. Phase Doppler measurements were performed through the transparent test window 2. The twenty thousand droplets of valid samples were obtained and analyzed for each measurement condition. The detailed optical parameters for the phase Doppler measurements are shown in Table 1.

Table 1. Optical configurations for phase Doppler measurements.

Optics		Specification
Transmitting optics	Ar$^+$ wavelength	514.5 nm
	Focal length	250 mm
	Spot diameter	233 µm
	Fringe spacing	3.21 µm
	Fringe number	72
Receiving optics	Focal length	310 mm
	Receiver aperture height	2.0 mm
	Frequency shift	40 MHz
	Scattering angle	30 degree
	Phase to conversion factor	0.955 µm/deg

2.3. Spectroscopic Water Detection

The wavelength must be set where the incident light is absorbed selectively by the water and passes through the gasoline, which follows the principles of spectroscopic water detection. The spectral absorbance of water and gasoline were measured using the spectrophotometer. In the spectroscopic measurement, a quartz cuvette was used as a sample container, and its path length was 1 cm. The spectral absorbance was measured over the wavelength range of λ = 200–1200 nm. Absorbance A is derived from transmittance T, which is the ratio of the intensity of transmitted light I_t to that of incident light I_0:

$$A = \log_{10}\left(\frac{1}{T}\right)$$ (1)

$$T = \frac{I_t}{I_0}$$ (2)

The optical model for the spectroscopic water detection in the gasoline pipe flow is indicated in Figure 2. The incident light is diminished through the water droplets, and the water content can be obtained by measuring the light transmittance. The light transmittance characteristics of the optical sensor model were predicted using the approximate light extinction theory of Mie scattering.

Figure 2. Optical model for spectroscopic water detection.
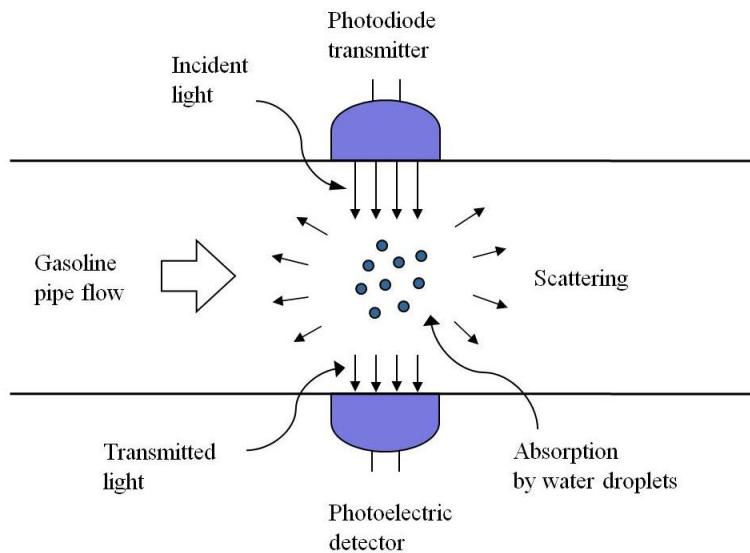
In the particles, the transmittance of Equation (2) is rewritten into Equation (3) using Bouguer's law [14]:

$$T = \frac{I_t}{I_0} = exp\left(-\sigma_e L\right)$$
(3)

where σ_e is the extinction coefficient of particles; and L is the path length of the light beam. If monodisperse particles are spherical and sufficiently lean:

$$\sigma_e = N A_p Q_e$$
(4)

where N is the number density of particles; A_p is the projected area of a particle; and Q_e is the extinction efficiency, which is the ratio of light power removed by particles to light power geometrically incident. The extinction efficiency Q_e is dependent on the optical properties of the refractive index and the shape and size of particles. If a particle is an absorbing material and the particle size is larger than the light wavelength, the extinction efficiency approaches $Q_e = 2$ by the light extinction theory of Mie scattering on particles, which follows Babinet's principle that the amount of light removed by diffraction is equal to that incident on the projected area of the particle [15,16].

In the calculation of extinction coefficient, the concept of mean diameters of droplets can be applied to the Equation (4). The definitions of mean diameters are expressed as follows [17]:

$$D_{pq} = \left[\frac{\sum D_i^{\,p} n_i}{\sum D_i^{\,q} n_i}\right]^{1/(p-q)}$$
(5)

where, i denotes the size range; n_i is the number of particles in size range i; D_i indicates the middle diameter of size range i; p and q are used for the determination of a particular diameter. In this equation, D_{10} is the arithmetic mean diameter; D_{20} is the surface mean diameter; D_{30} is the volume mean diameter; and D_{32} is the volume to surface mean diameter, which is also called the Sauter mean diameter.

The extinction coefficient of particles σ_e is expressed in terms of the surface mean diameter D_{20}, as follows:

$$\sigma_e = \pi N Q_e \frac{D_{20}^{\,2}}{4} \tag{6}$$

The volume concentration of particles C_v is expressed in terms of the volume mean diameter D_{30} as follows:

$$C_v = \pi N \frac{D_{30}^{\,3}}{6} \tag{7}$$

From the two Equations (6) and (7), the extinction coefficient of particles σ_e is expressed in terms of the volume concentration C_v and the Sauter mean diameter D_{32} as follows:

$$\sigma_e = \frac{3}{2} \frac{C_v\, Q_e}{D_{32}} \tag{8}$$

The Bouguer's equation for polydisperse particles is expressed as follows:

$$T = \frac{I_t}{I_0} = exp\left(-\frac{3}{2} \frac{C_v\, Q_e\, L}{D_{32}} \right) \tag{9}$$

In Equation (9), it is obvious that the transmittance dependents on the volume concentration C_v and Sauter mean diameter D_{32}. The volume concentration C_v can be obtained from the ratios of the water flow rate to the gasoline flow rate and Sauter mean diameter D_{32} are measured using phase Doppler measurement technique.

3. Results and Discussion

3.1. Water Droplet Characteristics

Figure 3 shows the images of the water droplet dispersion visualized by the CCD through the transparent window 2, which was installed downstream at about 70 times of the pipe hydraulic diameter away from the mixing device. The optical fiber stroboscope with the electric pulse duration of 10 µs was used as the back illuminating light source. The water contents of Figure 3a,b were $C_w = 100$ ppm, and the gasoline flow rates were $Q_g = 1.8$ m^3/h and 3.6 m^3/h, respectively. As shown in Figure 3a,b, the spherical water droplets dispersed and distributed almost homogeneous spatially. Therefore, it is regarded that the water droplets could be sufficiently permeated to the optical measurement. In this experiment, the water content was very small quantity 300 ppm and the gasoline flow was turbulent in the range of the Reynolds number $Re_g = 40{,}000$ to $80{,}000$. Therefore, the optical measurements were also permeable in the entire experiment.

Figure 4 shows the distributions of the arithmetic mean diameter D_{10} of water droplets along the transverse axis of the gasoline pipe flow. The droplet size distributions were measured by phase Doppler particle measurement system at the gasoline flow rates of $Q_g = 1.8$ m^3/h and $Q_g = 3.6$ m^3/h and water content $C_w = 150$ ppm. As illustrated in this figure, the distribution of droplet mean diameter showed lower values at higher gasoline flow rate because of hydrodynamic break-up effects. The

distributions of the mean diameters D_{10} showed approximately constant level with slight fluctuations. The standard deviations of the droplet distribution were about 4%. It can be seen that the water droplets were very well mixed with gasoline flow spatially.

Figure 3. Water droplet dispersion visualized through transparent test window 2: (**a**) $Q_g = 1.8$ m^3/h and $C_w = 100$ ppm; (**b**) $Q_g = 3.6$ m^3/h and $C_w = 100$ ppm.

(**a**)   (**b**)
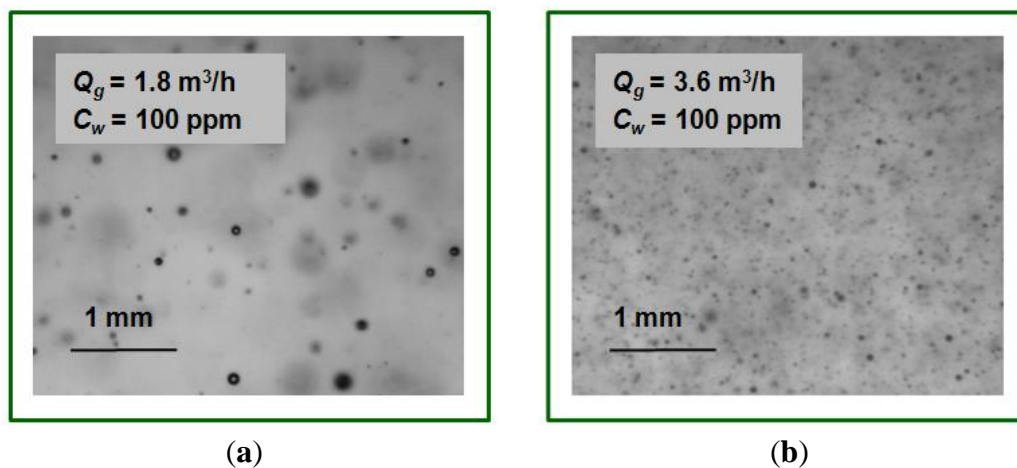
Figure 4. Distribution of arithmetic mean diameter of water droplets along transverse direction of gasoline pipe flow.
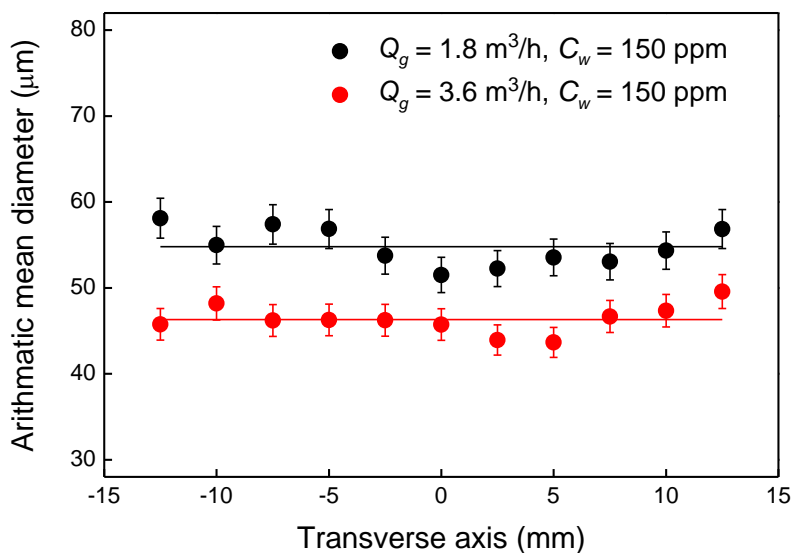
Figure 5a,b show the volume mean diameter D_{30} and number density N of water droplets. As shown in Figure 5a, the volume mean diameter D_{30} decreased with the increase of the water content and the gasoline flow rate. As shown in Figure 5b, the number density N of water droplets increased exponentially with increased water content at each gasoline flow rate, and the increasing rate of the number density N was gradually enlarged with increased gasoline flow rate. Therefore, it was regarded that the distribution of water droplets were sufficiently lean in the gasoline pipe flow.

Figure 5. Volume mean diameter and number density of water droplets: (**a**) volume mean diameter D_{30}; (**b**) number density N.

(**a**)   (**b**)
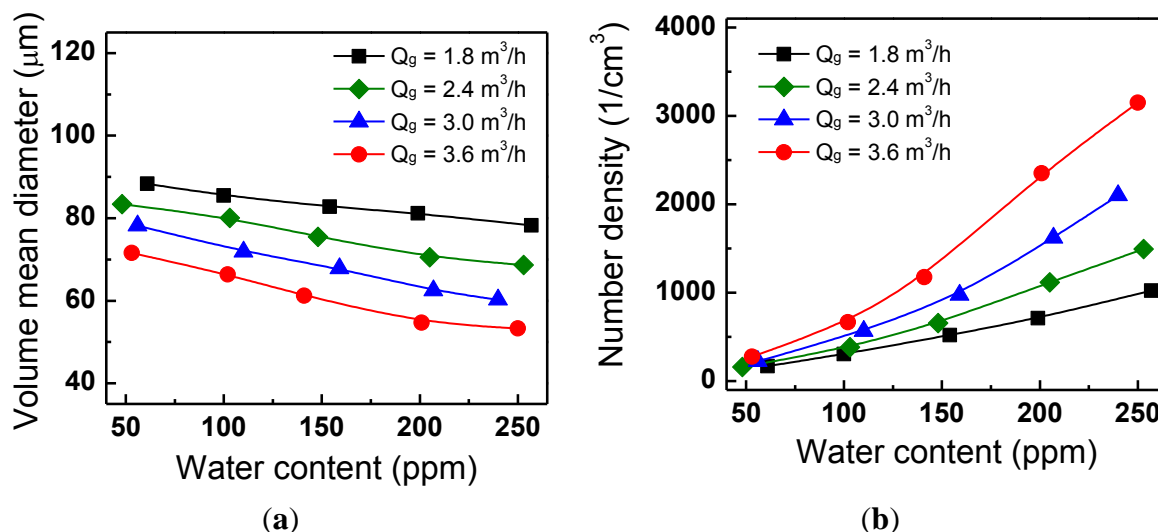
Figure 6a,b show distributions of size and cumulative volume of water droplets measured according to the flow rates at the water content C_w = 150 ppm. As shown in Figure 6a, when the gasoline flow rate varied from Q_g = 1.8 m³/h to Q_g = 3.6 m³/h, the number of small droplets increased and the number of large droplets decreased. The size distributions also shifted to small diameters. The arithmetic mean diameter D_{10} and Sauter mean diameter D_{32} decreased from D_{10} = 61 μm and D_{32} = 112 μm to D_{10} = 45 μm and D_{32} = 82 μm, respectively. As a result, the arithmetic mean diameter D_{10} and Sauter mean diameter D_{32} decreased by 26% and 27%, respectively. The cumulative volume distributions of water droplets are indicated in Figure 6b. In the case of the lower gasoline flow rate of Q_g = 1.8 m³/h, the cumulative volume of water droplets increased more rapidly in the range 150–180 μm. However, in the case of the higher gasoline flow rate of Q_g = 3.6 m³/h, the cumulative volume of water droplets increased rapidly in the range 50–100 μm. The median values of cumulative volume distributions decreased significantly by 37% from 135 μm to 85 μm when the gasoline flow rate increased from Q_g = 1.8 m³/h to Q_g =3.6 m³/h. It was understood that the flow rate of water and gasoline influenced hydrodynamic droplet break-up process and droplet atomization through the water supply nozzle and the mixing device [18].

Figure 7 shows the Sauter mean diameter D_{32} with the water content C_w according to gasoline flow rate Q_g. It was found that the Sauter mean diameter D_{32} decreased linearly with increased water content C_w and the decreasing rate with water content C_w was gradually enlarged with increased gasoline flow rate Q_g. When the water content varied from C_w = 50–250 ppm, the Sauter mean diameter D_{32} decreased by only about 5% at the lower gasoline flow rate of Q_g = 1.8 m³/h, but decreased significantly by 24% at the higher gasoline flow rate of Q_g = 3.6 m³/h. Consequently, it is believed that the effect of the water content on the Sauter mean diameter D_{32} of water droplets is significantly increased with the increase of the gasoline flow rate.

Figure 6. Distributions of size and cumulative volume of water droplets at $Q_g = 1.8$ m³/h, $C_w = 150$ ppm and $Q_g = 3.6$ m³/h, $C_w = 150$ ppm: (**a**) size distribution; (**b**) cumulative volume distribution.

(**a**)   (**b**)
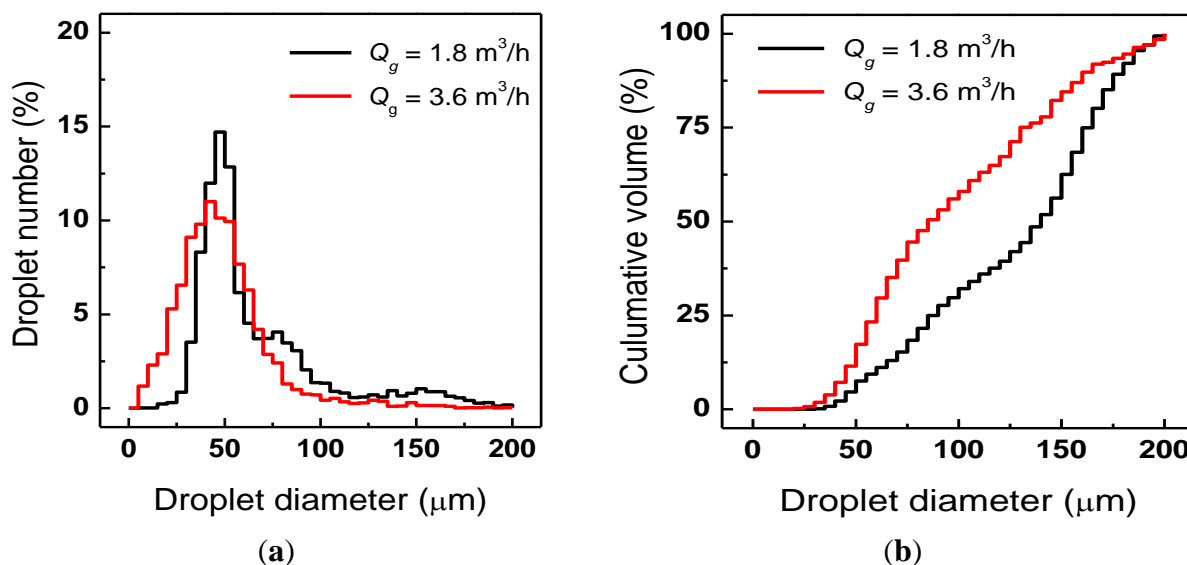
Figure 7. Sauter mean diameter of water droplets in gasoline pipe flow.
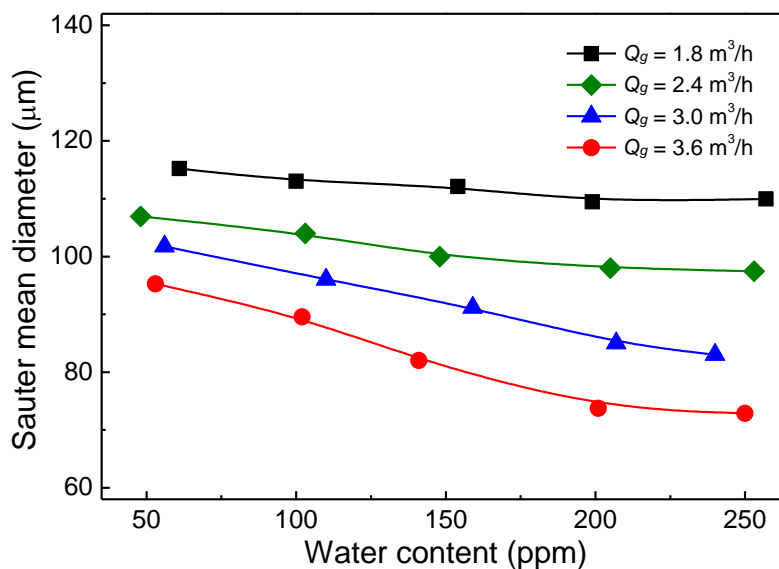
3.2. Spectroscopic Characteristics

Figure 8 shows the characteristics of spectral absorbance of water and gasoline. The spectral absorbance *A* was measured over a wavelength range of $\lambda = 200$ nm to 1200 nm. The measurement result of spectral absorbance showed that the absorbance of water was higher than that of gasoline only in the range of light wavelengths from $\lambda = 930$ nm to 1100 nm. The relative absorbance of water to gasoline was highest at the light wavelength of $\lambda = 980$ nm of a near-infrared ray, where the absorbance of water and gasoline were 0.73 and 0.07, respectively. As a result, gasoline was almost transparent to light at 980 nm wavelength while water showed absorption peak at this wavelength, therefore it was appropriate incident light for spectroscopic water detection.

Figure 8. Spectral absorbance characteristics of water and gasoline.
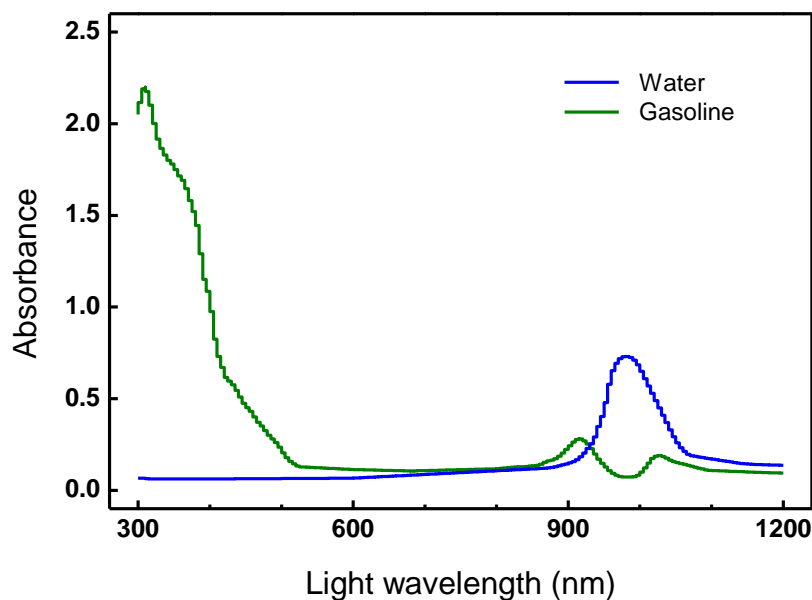
Figure 9a,b show the effect of water droplet diameter on the light transmittance characteristics under a quiescent condition of gasoline containing monodisperse water droplets using the Equation (9). For monodisperse droplets, all the mean diameters are same to a droplet diameter D. In Figure 9a, the transmittance T decreased linearly with increased water content and the decreasing rate with the water content was significantly enlarged with the decrease of the droplet diameter D. This result could be confirmed more clearly in Figure 9b, which showed that the light transmittance T increased logarithmically with the increase of the droplet diameter D, and the increasing rate was significantly enlarged with the increase of the water content C_w. However, the transmittance T in pipe flow would be different to that in this quiescent monodisperse droplet condition. In practical pipe flow, the droplet size would be dependent on the flow rates of gasoline and water as shown in Figure 7. Figure 10 indicates the effects of the flow rate of gasoline and water on the transmittance characteristics in practical gasoline pipe flow. The results showed that the light transmittance decreased linearly with increased water content and the decreasing rate of the light transmittance was gradually enlarged with increased gasoline flow rate. When the water content increased from $C_w = 50$–250 ppm, the light transmittance decreased by about 14% at a lower gasoline flow rate $Q_g = 1.8$ m^3/h, but the light transmittance decreased largely by about 21% at a higher gasoline flow rate $Q_g = 3.6$ m^3/h. As indicated in Figures 10, the light transmittance was significantly influenced by the gasoline flow rate Q_g and the water content C_w in the gasoline pipe flow. It was confirmed that the light transmittance characteristics were dependent on the Sauter mean diameter and the volume concentration of water droplets which were dependent on the gasoline flow rate and the water content.

Figure 9. Transmittance characteristics in quiescent gasoline containing monodisperse water droplets: (**a**) transmittance *versus* water content; (**b**) transmittance *versus* droplet diameter.

(**a**) (**b**)
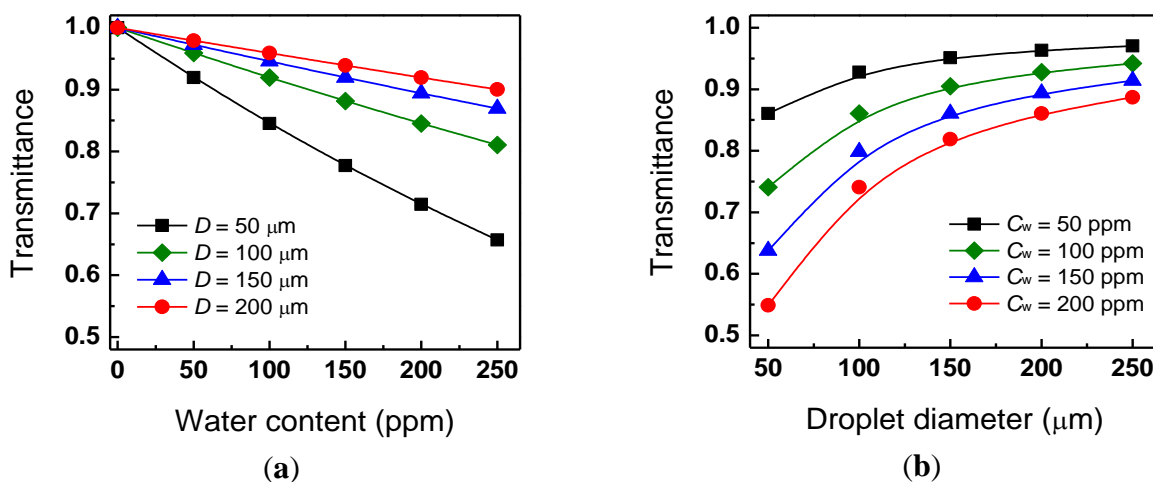
Figure 10. Transmittance characteristics in gasoline pipe flow.
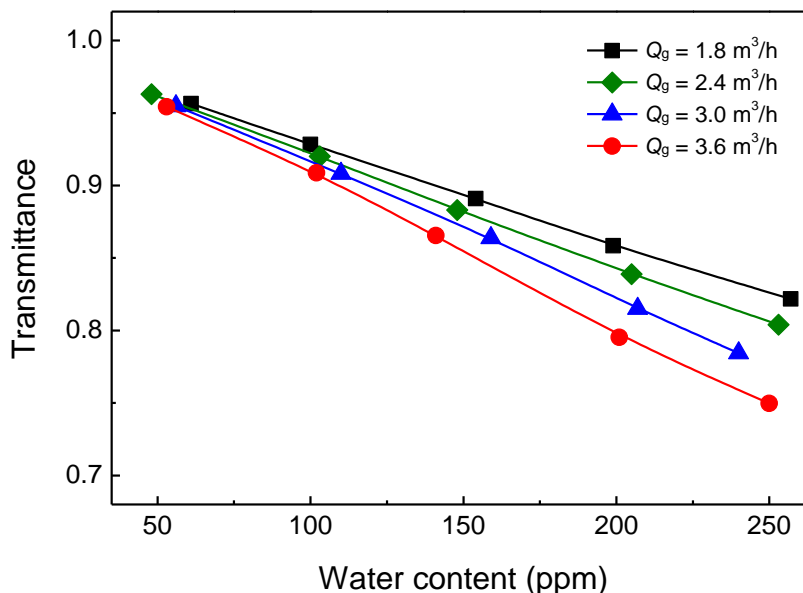
4. Conclusions

The hydrodynamic influence on spectroscopic water detection was investigated in a gasoline pipe flow. The effects of the flow rate of gasoline and water on the water droplet size were investigated experimentally, and the effects on the light transmittance were predicted by using the spectroscopic water detection. The water droplet content in gasoline varied within a range 50–250 ppm, and the gasoline flow rate varied within a range 1.8–3.6 m^3/h. The findings from the results are summarized as follows:

- In the gasoline pipe flow, the water from the nozzle disintegrated into small droplets by the hydrodynamic break-up mechanism through the mixing device, and the small spherical water droplets were sufficiently lean and dispersed almost homogeneously in the gasoline

pipe flow. The water droplet size was significantly decreased with the increase of the flow rate of gasoline and water. When the water content varied from 50 to 250 ppm, the Sauter mean diameter decreased by about 5% at the gasoline flow rate of 1.8 m^3/h, but decreased significantly by about 24% at the gasoline flow rate of 3.6 m^3/h.

- The measurement results of spectral absorbance showed that gasoline was almost transparent at 980 nm wavelength of light while water showed peak absorption at this wavelength. Therefore, it was appropriate incident light for spectroscopic water detection.
- The light transmittance decreased linearly with increased water content, and the decreasing rate of the light transmittance with the water content was also gradually enlarged with decreased gasoline flow rate. When the water content increased from C_w = 50 to 250 ppm, the light transmittance was reduced by about 14% at a lower gasoline flow rate of Q_g = 1.8 m^3/h, but it was reduced largely by about 21% at a higher gasoline flow rate of Q_g = 3.6 m^3/h.

In conclusion, the characteristics of light transmittance of gasoline and water provided an appropriate means for the optical water detection in a gasoline pipe flow. Also, the flow rate of gasoline and water influenced the Sauter mean diameter and the volume concentration of water droplets because the light transmittance was influenced by the flow rate of gasoline and water.

Acknowledgments

Author Contributions

In this study, Jeong Heon Kim contributed to the design and the experiment of spectroscopic water detection in gasoline pipe flow and writing the manuscript. Chang Sik Lee analyzed the investigation results of water flow in the gasoline pipe and spectral absorbance of water and gasoline. He investigated the relationships between droplet size and water content in gasoline pipe flow and wrote the manuscript of this paper.

Conflicts of Interest

The authors declare no conflict of interest.

References

1. Gong, J.-S.; Fu, W.-B. A Study on the effect of more volatile fuel on evaporation and ignitionfor emulsified oil. *Fuel* **2001**, *80*, 437–445.
2. Fu, W.-B.; Hou, L.-Y.; Wang, L.-P.; Ma, F.H.A. Study on ignition characteristics of emulsified oil containing flammable fuel. *Fuel Process. Technol.* **2003**, *80*, 9–21.
3. Alahmer, A. Influence of using emulsified diesel fuel on the performance and pollutants emitted from diesel engine. *Energy Convers. Manag.* **2013**, *73*, 361–369.

4. Attia, A.M.A.; Kulchitskiy, A.R. Influence of the structure of water-in-fuel emulsion on diesel engine performance. *Fuel* **2014**, *116*, 703–708.

5. Huo, M.; Lin, S.; Liu, H.; Lee, C.F. Study on the spray and combustion characteristics of water–emulsified diesel. *Fuel* **2014**, *123*, 218–229.

6. Chantrapornchai, W.; Clydesdale, F.; Julian, D.M. Influence of droplet characteristics on the optical properties of colored oil-in-water emulsions. *Colloids Surf. A* **1999**, *155*, 373–382.

7. Bae, C.; Kim, J.H.; Sheen, D.H. *Optical Measurements of Water Droplet Characteristics in Turbulent Gasoline Pipe Flow*; SAE Technical Paper 2001-01-1965, SAE International: Orlando, FL, USA, 2001.

8. Bampi, M.; Scheer, A.P.; Castilhos, F. Application of near infrared spectroscopy to predict the average droplet size and water content in biodiesel emulsions. *Fuel* **2013**, *113*, 546–552.

9. Bohren, C.F.; Huffman, D.R. *Absorption and Scattering of Light by Small Particles*; John Wiley & Sons: New York, NY, USA, 1999.

10. Hinds, W.C. *Aerosol Technology*, 2nd ed.; John Wiley & Sons: New York, NY, USA, 1999.

11. Naqwi, A.A.; Durst, F. Light scattering applied to LDA and PDA measurements. *Part. Part. Syst. Charact.* **1991**, *8*, 245–258.

12. Kim, J.H.; Ikeda, Y.; Nakajima, T. Characteristic Measurements of Electrostatic Fuel Spray. In Proceedings of 9th International Symposium on Applications Laser Techniques to Fluid Mechanics, Lisbon, Portugal, 13–16 July 1998; pp. 21.5.1–21.5.6.

13. Kim, J.H.; Nakajima, T. Aerodynamic influences on droplet atomization in an electrostatic spray. *JSME Int. J. Ser. B* **1999**, *42*, 224–229.

14. Ingle, J.D.; Crouch, R. *Spectrochemical Analysis*; Prentice Hall: Englewood Cliffs, NJ, USA, 1988.

15. Yin, J.; Pilon, L. Efficiency factors and radiation characteristics of spherical scatters in an absorbing medium. *J. Opt. Soc. Am. A* **2006**, *23*, 2784–2796.

16. Sudiarta, I.W.; Chylek, P. Mie scattering efficiency of a large spherical particle embedded in an absorbing medium. *J. Quant. Spectrosc. Radiat. Transf.* **2001**, *79*, 709–714.

17. Mugele, R.A.; Evans, H.D. Droplet size distribution on spray. *Ind. Eng. Chem.* **1951**, *43*, 1317–1324.

18. Lee, C.S.; Reitz, R.D. Effect of liquid properties on the breakup mechanism of high-speed liquid drops. *At. Sprays* **2001**, *11*, 1–19.